High-pressure Raman investigation of mutual solubility and compound formation in Xe-N2 and Ne-N2

High-pressure Raman investigation of mutual solubility and compound formation in $Xe\text{-}N_2$ and $Ne\text{-}N_2$

M. E. Kooi* and J. A. Schouten†
Van der Waals–Zeeman Institute, University of Amsterdam, Valckenierstraat 65, 1018 XE Amsterdam, The Netherlands
(Received 25 January 1999; revised manuscript received 15 June 1999)

In this study, the mixed solid phases of the molecular systems $Xe\text{-}N_2$ and $Ne\text{-}N_2$ have been investigated up to 13 GPa using Raman spectroscopy and so-called $\nu\text{-}T$ and $p\text{-}T$ scans. Both systems show a rich variety of solid phases. In $Xe\text{-}N_2$ a van der Waals compound has been found. The solubility of N_2 in solid Xe is about 7.5 mol %, while the solubility of the larger Xe atoms into the β and δ phases of N_2 is higher. In $Ne\text{-}N_2$ two van der Waals compounds have been detected. The Raman spectrum of one of these compounds is very similar to that of $He(N_2)_{11}$. N_2 does not dissolve into solid Ne, while Ne does dissolve into the β and δ phases of N_2, even though the atomic diameter of Ne is considerably smaller than the molecular one of N_2. Analogous to $Ar\text{-}N_2$, the Ne and Xe atoms are mainly located at the *a* sites in the δ^* phase. For $Ne\text{-}N_2$, in contrast to $Xe\text{-}N_2$, the $\beta^*\text{-}\delta^*$ transition shifts to higher pressure. The $\varepsilon^*\text{-}\delta^*$ transition is not shifted for $Ne\text{-}N_2$. The results have been compared with computer simulations and analytical theories for hard-sphere systems. It is shown that the ratio of the diameters of the molecules, α, is only a very rough indication for the phase behavior of mixed molecular systems at high pressure. [S0163-1829(99)08641-5]

INTRODUCTION

In molecular systems the introduction of a second component leads to interesting phenomena like the formation of van der Waals compounds, orientational glasses, and disordered mixed solids. The properties of these new solids are quite different from those of the constituting components. In addition, phase lines can shift enormously, so that certain high-pressure phases can be formed at considerable lower pressures in the mixed system, and other phases might not be formed at all.

The literature about the mutual solubility of simple molecular systems in the solid phase is rather limited. More work has been done on metallic systems. It is generally believed that solubility at high density, in particular in solid systems, is mainly governed by geometrical effects, as expressed by the well-known Hume-Rothery rule.[1] This empirical rule states that a binary mixed solid is obtained only if the ratio of the diameters of the molecules, α, is larger than 0.85. As long as the mixed solid is completely disordered, the Hume-Rothery rule is in fair agreement with computer simulations[2] and analytical theories.[3,4] In addition, the simulations show that the solubility of large spheres in the solid formed by small spheres is much smaller than vice versa. We will investigate whether these geometrical rules are also valid for molecular systems.

When the molecular diameters of the two components differ considerably, stoichiometric compounds can be formed. For hard-sphere systems[5–8] these compounds (AB, AB_2, and AB_{13}) are stabilized by the entropy and efficient packing.

Up to now, a number of compounds have been found in molecular systems. Because the interactions between the molecules are of the van der Waals type, these solids are called van der Waals compounds. In the literature the occurrence of these van der Waals compounds is often explained by efficient packing of hard spheres, dictated mainly by α (see, e.g., Ref. 9). In this work we will investigate if this is indeed the case (see also Ref. 10).

Binary mixtures of nitrogen and a noble gas are suitable model systems for the following reasons. The nitrogen molecule is a simple diatomic slightly nonspherical molecule, the interaction potential is well known, and pure nitrogen has been studied extensively (see, e.g., Ref. 11 and references therein). It provides a good opportunity to investigate the effect of asphericity and weak intermolecular forces on the mutual solubility and compound formation. Moreover, nitrogen has a peculiar high-pressure phase, the δ phase ($Pm3n$), in which the molecules on the *a* sites are completely orientationally disordered (spheres), whereas the molecules on the *c* sites are orientationally disordered only in a plane normal to the faces of the unit cell (disks). The system shows a second-order transition, δ_{rot} to δ_{loc}.[12]

Previous investigations of $He\text{-}N_2$ and $Ar\text{-}N_2$ revealed a very complex phase behavior for these mixtures. In $He\text{-}N_2$ ($\alpha = 0.62$), a disordered solid solution exists at high pressure and low temperature on the nitrogen-rich side of the phase diagram.[13,14] A stoichiometric compound [$He(N_2)_{11}$] has been detected at room temperature.[15] The Raman spectrum of the compound is very similar to that of $\varepsilon\text{-}N_2$,[16,17] but the intensity ratio between the two Raman peaks ν_1 and ν_2 is decreased compared to the spectrum of pure $\varepsilon\text{-}N_2$.

The high-pressure investigations on the mixture $Ar\text{-}N_2$ (Refs. 18 and 19) ($\alpha = 0.95$, with nitrogen the larger molecule) show that the solubility of argon in the solid β and δ phases of nitrogen is very high. The Raman spectra reveal that the argon atoms have a preference for the *a* sites in the δ phase. The distribution of the argon atoms over the sites is temperature and pressure dependent. The $\delta\text{-}\varepsilon$ transition has not been found experimentally in the mixed system. As shown by computer simulations, it probably shifts towards lower temperatures or higher pressure by the addition of argon.[20]

In order to study the evolution of the phase diagram, the mutual solubility, and the compound formation as a function of α in nitrogen systems, we have studied the phase diagrams of Ne-N_2 ($\alpha=0.74$) and Xe-N_2 ($\alpha=0.89$).

We will present Raman measurements as a function of pressure up to 13 GPa. In addition, so-called ν-T and p-T scans will be performed for Ne-N_2. Finally, phase diagrams for these mixtures will be proposed and the results will be discussed.

EXPERIMENTAL RESULTS

Xe-N_2 mixtures, with nitrogen mole fractions x of 0.075 and 0.84 and Ne-N_2 mixtures with $x=0.90$, 0.35, and 0.052 have been prepared in a gas compressor. The experimental procedure has been described elsewhere.[19] The pressure is determined by the ruby luminescence method using the pressure scale of Ref. 21 and the temperature correction of Ref. 22. The Raman spectra have been fitted by Lorentzian curves. These curves are used to determine the peak position and the full width at half maximum (FWHM). The instrumental width is about 0.75 cm^{-1}.

In all cases, only one single Raman peak (ν_F) has been observed at low pressures in the fluid phase, as could be expected. Observations through the microscope show that the sample space is completely transparent under these conditions. In addition, visual observations show the appearance of a solid phase when the pressure is increased.

As is shown by visual observations, usually we do not obtain a fine-grained phase-separated mixture, but larger pieces (compared to the focal cylinder of the laser) of the individual solid phases are formed. Therefore, when the laser is focused at different spots in the sample space and the intensity ratio between Raman peaks does not change, it is assumed that these peaks are all modes of one single solid phase. Important information is also obtained from the linewidth, since it is not only a function of pressure, but it also depends strongly on the composition. Moreover, the linewidth is much smaller in a solid than in a liquid at the same pressure and temperature.

Xe-N_2

The measurements have been performed at constant temperature (408 K). Typical Raman spectra are shown in Figs. 1 and 2. The vibrational frequency as a function of pressure is presented in Fig. 3.

For $x=0.84$, at the fluid solid transition (4.9 GPa), a drastic drop of the linewidth occurs similar to that observed for pure N_2.[23] For $p\geq 4.9$ GPa, the Raman spectrum consists of two peaks as shown in the lower spectrum of Fig. 1. For reasons to be explained later, the high-frequency peak is referred to as $\nu_{\beta*}$ and the low-frequency peak as ν_F. At 6.0 GPa three additional vibrational modes were measured (Fig. 1) indicating a three-phase equilibrium. The additional modes consist of one peak on the high-frequency side of $\nu_{\beta*}$ ($\nu_{1a\delta*}$) and two peaks on the low-frequency side of $\nu_{\beta*}$ ($\nu_{2a\delta*}$ and $\nu_{2b\delta*}$). Above 6.0 GPa, ν_F and $\nu_{\beta*}$ could no longer be detected, but an additional peak ($\nu_{1b\delta*}$) below $\nu_{1a\delta*}$ was found. The four peaks are all modes of one single phase (δ*). The intensity of the peaks $\nu_{1a\delta*}$, $\nu_{1b\delta*}$, and

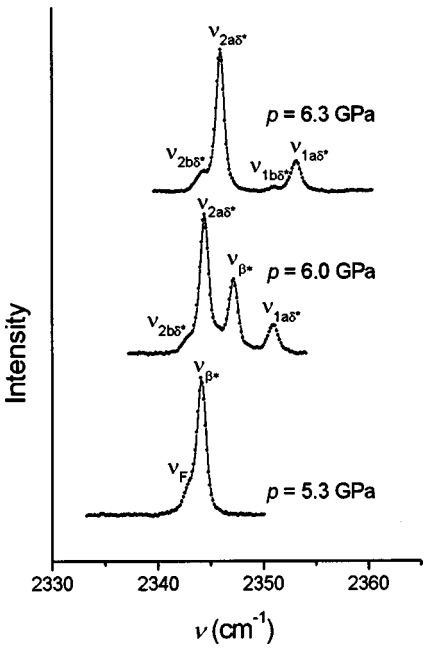

FIG. 1. Typical Raman spectra of N_2 in Xe-N_2, $x=0.84$.

$\nu_{2b\delta*}$ divided by that of $\nu_{2a\delta*}$ is, respectively, 0.25 ± 0.02, 0.03 ± 0.01, and 0.06 ± 0.03. The mode $\nu_{1b\delta*}$ is no longer detectable above 9.8 GPa.

For $x=0.075$ coexisting solid and fluid phases have been observed above 0.83 GPa. The amount of solid increases at increasing pressure, until the sample space seems to be completely filled with solid. A typical Raman spectrum of the fluid phase is represented by the lower spectrum in Fig. 2. Note that the small peak at about 2330 cm^{-1} (ν_0) is the Raman peak of N_2 in the ambient air. Above the fluid-solid transition two vibrons are observed as shown at 1.4 GPa in Fig. 2. One can clearly observe that the distance between these two peaks increases as a function of pressure due to a rapid increase of ν_F. Above 1.6 GPa the high-frequency

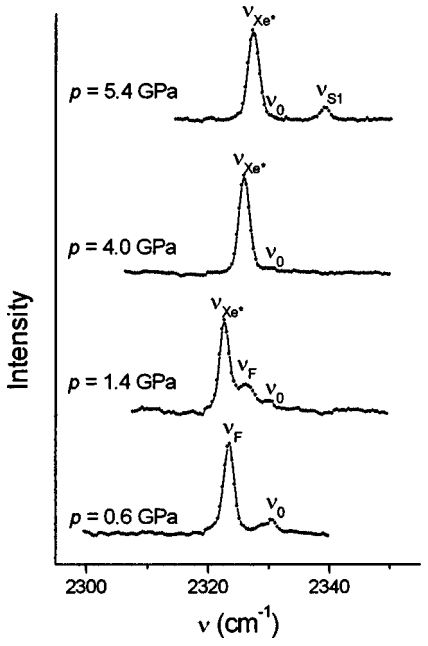

FIG. 2. Typical Raman spectra of N_2 in Xe-N_2, $x=0.075$.

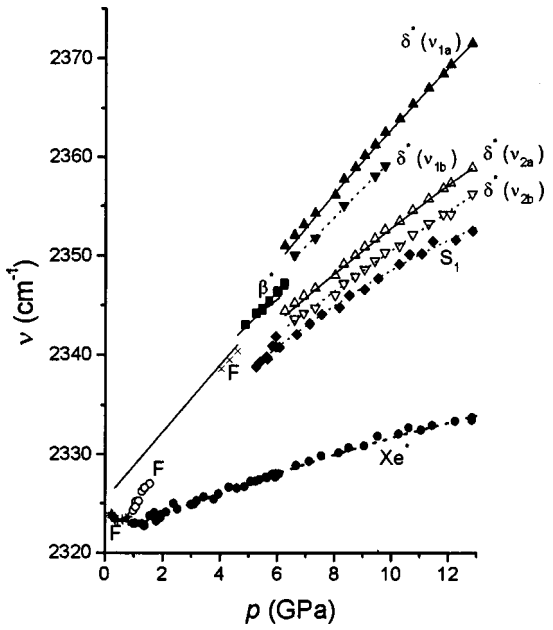

FIG. 3. Raman frequency vs pressure of N_2 in Xe-N_2 at 408 K. $x=0.84$: crosses, homogeneous fluid; squares, $\nu_{\beta*}$; triangles, modes of δ*. $x=0.075$: plus signs, homogeneous fluid: open circles, fluid in coexistence region; solid circles, $S_{\mathrm{Xe}*}$; diamonds, S_1. Solid lines represent the extrapolated frequencies of the fluid (Ref. 33), β and δ phases of pure N_2 at 408 K (Ref. 36). Dotted lines are guides to the eyes.

peak is no longer detectable. At 5.3 GPa a new peak appears (ν_{S1}), with a frequency about 12 cm^{-1} higher than $\nu_{\mathrm{Xe}*}$ (upper spectrum in Fig. 2). One can observe in Fig. 3 that ν_{S1} increases slightly more as a function of pressure than $\nu_{\mathrm{Xe}*}$.

Ne-N_2

1. Constant temperature measurements

The measurements have been performed at room temperature (296 K), except for one experimental run which was performed at 408 K. Typical Raman spectra are given in Fig. 4. The frequency and linewidth as a function of pressure are presented in Figs. 5 and 6, respectively.

For $x=0.052$, 0.35, and 0.90, the solid-fluid coexistence region is reached, respectively, at 5.29, 7.71, and 4.44 GPa at room temperature. For $x=0.052$ and 0.35, in the solid-fluid coexistence region, still only one Raman peak is observed as shown at 8.0 GPa in Fig. 4. There is no discontinuity in the peak position or in the FWHM of the Raman spectrum at the entrance point to the solid-fluid region. In the solid-fluid coexistence region the values of the peak position and of the FWHM, and their pressure dependence, are the same for the mixtures $x=0.052$ and 0.35. Therefore, the Raman peak in the coexistence region is attributed to the fluid phase. Thus nitrogen does not dissolve in solid neon.

For the mixture with $x=0.052$, these experiments were also performed at 408 K; essentially the same behavior was observed. At this temperature, the solid-fluid coexistence region is entered at 8.3 GPa.

For $x=0.90$, the Raman spectrum consists of two peaks (ν_F and $\nu_{\beta*}$) in the solid-fluid coexistence region. The Raman frequency of β* is 0.2 cm^{-1} higher than that of pure β-N_2 in the stability range of β-N_2. The broad Raman peak ν_F is present until at least 7.5 GPa, but we could not find the fluid peak for 5.4 GPa$<p<$7.5 GPa possibly because of the low amount of fluid present in the sample space.

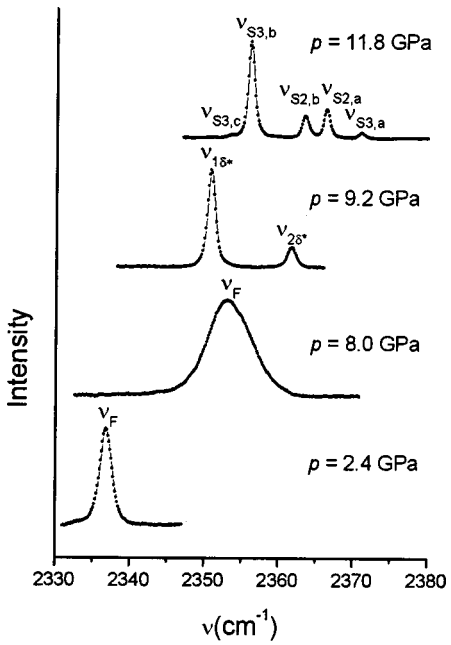

FIG. 4. Raman spectra of N_2 in Ne-N_2 at 296 K, $x=0.35$.

Increasing the pressure, in the mixture with $x=0.052$, in addition to ν_F, two new modes appear ($\nu_{S2,a}$ and $\nu_{S2,b}$) at 8.35 GPa at the high-frequency side of ν_F. The intensity

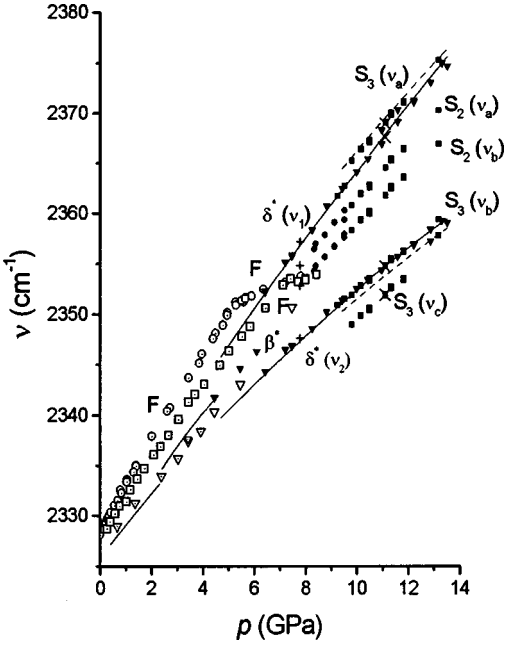

FIG. 5. Raman frequency vs the pressure of N_2 in Ne-N_2 at 296 K. Circles, $x=0.052$; squares, $x=0.35$; triangles, $x=0.90$, open symbols with dot, fluid in homogeneous region; open symbols without dot, fluid in coexistence region; plus signs ($x=0.35$) and crosses ($x=0.90$), Raman frequencies obtained at 296 K in a heating scan. Solid lines represent the frequencies of the fluid (Ref. 33), β and δ phases of pure N_2, respectively (Ref. 36) and dashed lines the extrapolated frequencies of pure ε-N_2 at 296 K (Ref. 36).

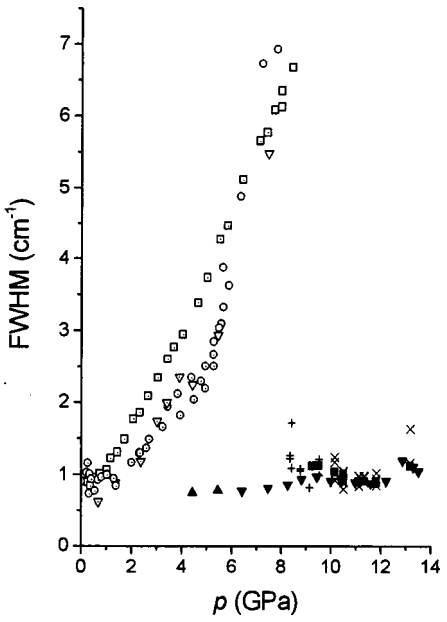

FIG. 6. FWHM vs the pressure of the Raman peak of N_2 in Ne-N_2 at 296 K. Circles, $x=0.052$: squares, $x=0.35$; triangles, $x=0.90$; open symbols with dot, fluid in homogeneous region; open symbols without dot, fluid in coexistence region; solid up triangles, $\beta^*(x=0.90)$; solid down triangles ($x=0.90$), $S_2(\nu_b)$ and $S_3(\nu_b)$; solid squares ($x=0.35$), $S_2(\nu_b)$ and $S_3(\nu_b)$; plus signs ($x=0.052$), modes of S_2: crosses ($x=0.35$), modes of S_2. For the sake of clarity the linewidths of the other modes have not been plotted.

ratio of $\nu_{S2,a}$ and $\nu_{S2,b}$ is about 1.2. No change has been observed by visual observations at 8.35 GPa. Similar modes have also been measured at and above 9.8 GPa in the mixture with $x=0.35$. For $x=0.052$ and 0.35 the modes have been measured up to 9.5 and 13.2 GPa, respectively, the highest pressures achieved for these mixtures.

Increasing the pressure in the mixture with $x=0.35$, there is no longer a ν_F peak at 9.2 GPa, but two new peaks have been found ($\nu_{1\delta*}$ and $\nu_{2\delta*}$), with an intensity ratio of 0.24 ± 0.03, as shown in Fig. 4. Through the microscope two different solid phases can be observed. The other solid, which can be observed by visual observations, is not Raman active and must be pure neon. The Raman frequencies $\nu_{1\delta*}$ and $\nu_{2\delta*}$ can be measured until at least 9.51 GPa. The intensity ratio remains constant over this pressure range. When increasing the pressure further, a change in the Raman spectrum has been observed at 9.8 GPa. The spectrum now consists of five new peaks. Two of these peaks are the modes of S_2, which were already mentioned before. The other three peaks will be referred to as $\nu_{S3,a}$, $\nu_{S3,b}$, and $\nu_{S3,c}$. The intensity ratio between $\nu_{S3,a}$ and $\nu_{S3,b}$ is equal to 0.07 ± 0.01 and that between $\nu_{S3,c}$ and $\nu_{S3,b}$ is 0.03 ± 0.01. The frequency of $\nu_{S3,b}$ is within experimental accuracy the same as the extrapolated frequency $\nu_{2\delta*}$. The mode $\nu_{1\delta*}$ is no longer detected.

In the mixture with $x=0.90$ at 11.0 GPa, an additional peak appears on the high-frequency side of $\nu_{1\delta*}$, which is referred to as $\nu_{S3,a}$, since the frequency is the same as that observed for $x=0.35$. The spectrum consists of three peaks, namely, $\nu_{S3,a}$, $\nu_{1\delta*}$, and $\nu_{2\delta*}$. One would also expect to measure $\nu_{S3,c}$, but the intensity of this peak is possibly too low to be detected. Above 11.6 GPa, $\nu_{S3,a}$ is no longer detected.

2. ν-T and p-T scans

In order to obtain more information about the character of the various solid phases, we have also performed scans of ν and p against temperature for $x=0.35$ and 0.90 in steps of about 5 K. This is a very suitable method to detect three-phase lines in binary systems, since generally at a three-phase line the pressure increases or decreases sharply and/or a drastic change is observed in the Raman spectrum. The formation of the various solid phases in Ne-N_2 shows a large metastability or hysteresis. When, for example, for $x=0.35$ the temperature was decreased at 7.8 GPa until 220 K and then increased again, the modes of δ^* and S_2 were measured at room temperature (+ in Fig. 5), while along the room-temperature isotherm the homogeneous fluid was still present up to 8.4 GPa. Because of the metastability, for each scan the temperature was first decreased until well below the starting point of the scan. All the transition lines given in this work have been obtained on heating.

$x=0.35$. Five scans have been measured for 7.5 GPa$\leqslant p \leqslant$11.5 GPa. Two typical scans at about 10 GPa are presented in Figs. 7(a) and 7(b). At low temperatures, the Raman spectrum is similar in shape to that measured for $p\geqslant 9.80$ GPa at room temperature. The peak $\nu_{S3,b}$ shows an asymmetry on the high-frequency side, as shown in Fig. 8 (marked by an arrow). When increasing the temperature, an additional peak appears on the low-frequency side of $\nu_{S3,a}$ [at 300 K in Fig. 7(b)], which is identified as $\nu_{1\delta*}$. Since at this temperature three different phases are present, it is identified as a point on the three-phase line S_3-S_2-δ^* (Fig. 9). The pressure increases slightly at this particular temperature. When further increasing the temperature, first the modes of S_3 disappear, then the two peaks of δ^* disappear, and a small broad peak appears, ν_F. This temperature is identified as a point on the three-phase line S_2-δ^*-F (Fig. 9). We were unable to determine the frequency ν_F for all temperatures. At even higher temperatures, the pressure increases sharply as shown in Fig. 7(a). For reasons to be explained later, this line is denoted as S_2-F-$S_{\mathrm{Ne}*}$. Note that the Raman frequencies also increase at this three-phase line [Fig. 7(b)], due to the increase of the pressure. When further increasing the temperature, visual observations show the melting of a solid ($S_{\mathrm{Ne}*}$). This solid is not Raman active and, therefore, must be pure neon. The temperature is now increased very slowly to determine the temperature of the final solid disappearance ($S_{\mathrm{Ne}*}$-F point) accurately by visual observations. In Fig. 7(b) these points are marked by arrows. No discontinuity of the Raman frequency occurs within experimental accuracy at the $S_{\mathrm{Ne}*}$-F point. In addition, the FWHM also does not show a discontinuity at this temperature.

$x=0.90$. One heating scan has been performed around 11 GPa. The frequencies have been compared in Fig. 10 with those obtained from a heating scan for $x=0.35$ at the same pressure, starting at 278 K. As shown in Fig. 8, a small wing (marked by arrow) on the high-frequency side of $\nu_{S3,b}$ is visible. Above 196 K the mode $\nu_{1\varepsilon*}$ is no longer detectable. When the laser is focused at a different spot in the sample space, the intensity of $\nu_{S3,a}$ increases slightly, while the in-

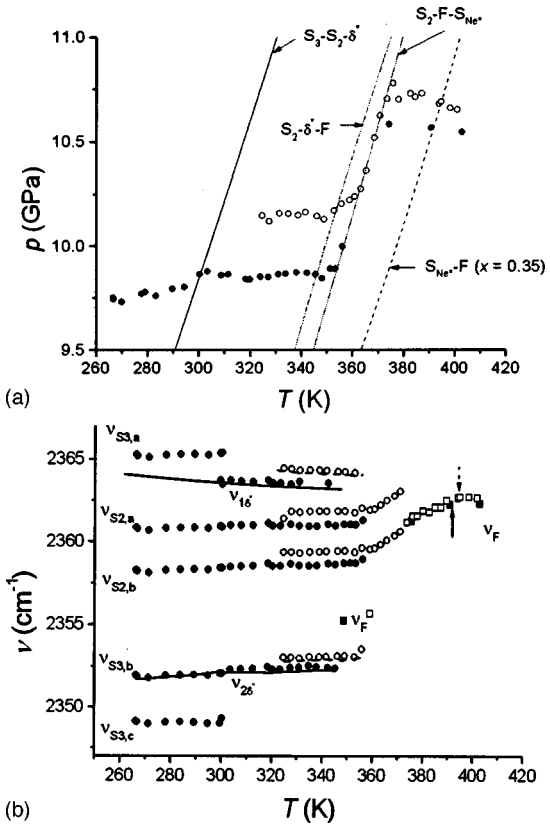

FIG. 7. (a) Typical p-T scans for $x=0.35$ (circles). Lines are transition lines given in Fig. 8. (b) Simultaneous typical ν-T scans for $x=0.35$. Circles, Raman frequencies of solid phases, squares Raman frequencies of fluid phase. Open symbols, ν-T scan at slightly higher pressure; solid symbols, ν-T scan at slightly lower pressure. Dashed and solid lines, Raman frequencies of pure δ-N_2 at the corresponding temperature and pressure (Ref. 36); arrows, $S_{Ne*}F$ points for these two scans, measured by visual observations. Solid lines, low-pressure scan; dashed lines, high-pressure scan.

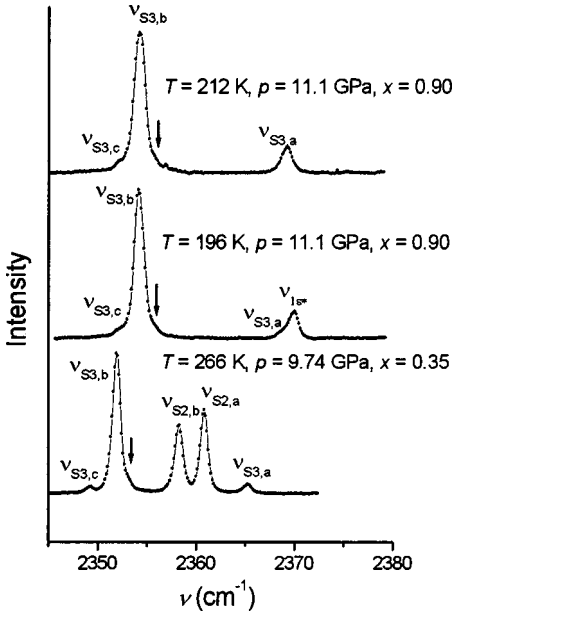

FIG. 8. Comparison between spectra for $x=0.90$ and $x=0.35$.

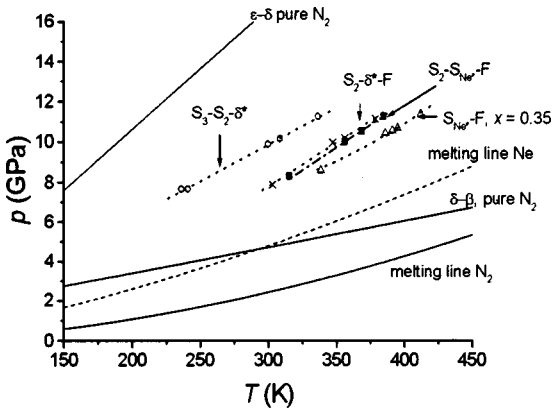

FIG. 9. An overview of the temperature scans for Ne-N_2. Circles, S_3-S_2-δ* three-phase line; crosses, S_2-δ*-F three-phase line; squares, S_2-S_{Ne*}-F three-phase line; triangles, $S_{Ne*}F$ line for $x=0.35$. Solid lines, transition lines of pure N_2 (Refs. 17 and 24); dashed line, melting line of Ne (Ref. 37). Dotted and dash-dotted lines are fits through the points on the transition lines.

tensity of $\nu_{S3,c}$ decreases slightly and vice versa. The intensity ratio of $\nu_{S3,a}$ and $\nu_{S3,b}$ is much larger than for $x=0.35$. In contrast to the results for $x=0.35$, for $x=0.90$, the modes of S_2 have not been detected at low temperature. The two peaks which appear at 310 K ($\nu_{S2,a}$ and $\nu_{S2,b}$) have a very low intensity.

SUGGESTED PHASE DIAGRAMS

The suggested phase diagrams have been presented in Figs. 11 and 12. In the following we will explain how these diagrams have been constructed.

Xe-N_2

For $x=0.84$, the solid-fluid coexistence region is entered at 4.9 GPa, which is 0.3 GPa above the melting line of pure N_2.[24] In the coexistence region ν_F corresponds to the extrapolated frequency of the homogenous fluid. Therefore, ν_F is attributed to the fluid phase and, consequently, $\nu_{\beta*}$ to the Raman mode of N_2 in the solid phase. There is no difference between the value of $\nu_{\beta*}$ and the Raman frequency of pure β-N_2 (Fig. 3). This suggests that pure β-N_2 and the β* phase in the mixture are closely related. In the coexistence

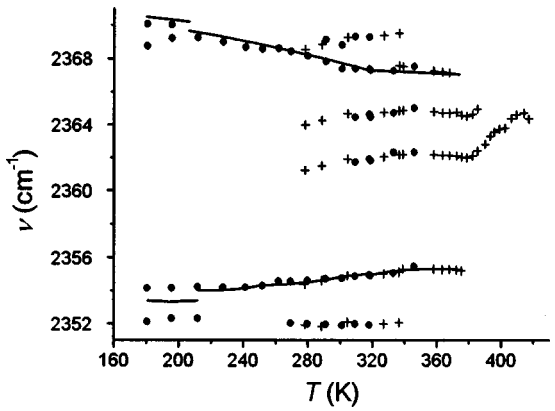

FIG. 10. ν-T scan for $x=0.90$ at 11 GPa, compared with a scan for $x=0.35$ at the same pressure. Circles, $x=0.90$; crosses, $x=0.35$. Solid lines are the frequencies of pure ε- and δ-N_2 (Ref. 36).

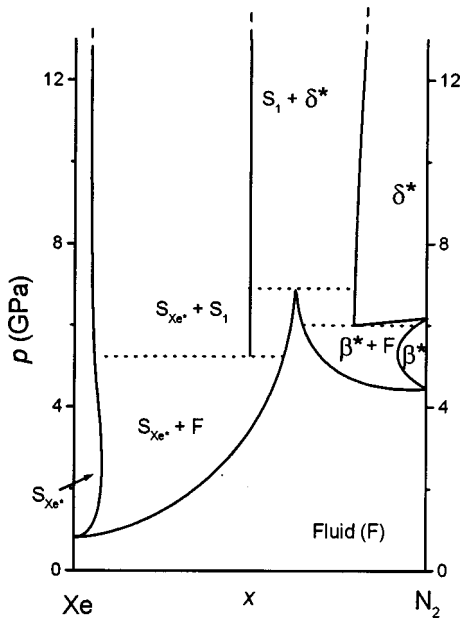

FIG. 11. Suggested p-x phase diagram for Xe-N_2 at 408 K.

region, at the entrance point, the intensity of ν_F is already quite low, which can be explained by metastability. Since when the laser is focused on different spots in the sample space the intensity of ν_{β^*} is always high compared to that of ν_F, a considerable amount of β^* must be present in the sample space. Therefore, a large amount of Xe dissolves into the β^* phase, probably more than the amount of nitrogen that dissolves into solid Xe (see $x=0.075$).

At 6.0 GPa a phase transition occurs to the δ^* phase, since at 6.0 GPa, simultaneously ν_{β^*} and the high-pressure modes $\nu_{1a\delta^*}$, $\nu_{2a\delta^*}$, and $\nu_{2b\delta^*}$ were measured. There is no deviation between $\nu_{1a\delta^*}$ and $\nu_{2a\delta^*}$, and ν_1 and ν_2 of pure δ-N_2. Therefore, we propose that this new phase (δ^*) is a mixed solid of Xe dissolved into the δ phase of N_2. In the mixture, the β^*-δ^* transition is slightly shifted to lower pressures, since for pure N_2 the transition occurs at 6.2 GPa at 408 K.[24] Because no other high-pressure phases have been detected for $x=0.84$, it is concluded that more than 16 mol % Xe dissolves into δ-N_2. In contrast to δ^*, the δ phase of pure N_2 has only two Raman-active modes ν_1 (a sites) and ν_2 (c sites). Since the unit cell contains 3 times as much c sites as a sites, the intensity ratio of ν_1 and ν_2 is 0.33. For $x=0.84$ the ratio of the sum of the integrated intensities $\nu_{1a\delta^*}$ and $\nu_{1b\delta^*}$ and the sum of the integrated intensities $\nu_{2a\delta^*}$ and $\nu_{2b\delta^*}$ is 0.28 ± 0.03. This suggests a preference of the Xe atoms for the a sites in the mixed solid δ^*.

For the mixture with $x=0.075$, the solid-fluid region is entered at 0.83 GPa, which is close to the estimated melting pressure of Xe from an extrapolation of the data of Ref. 25. In the solid-fluid coexistence region, the intensity of ν_F decreases as a function of pressure compared to that of ν_{Xe^*}. Therefore, ν_F is attributed to the fluid phase and, consequently, ν_{Xe^*} to the Raman mode of N_2 in the mixed solid phase. It is concluded that N_2 dissolves into solid Xe (fcc). The rapid increase of ν_F as a function of pressure can be explained by a rapid change in composition of the fluid phase. This is reflected in the liquidus of Fig. 11. The absence of a fluid peak above 1.6 GPa suggests that (nearly) all the nitrogen dissolves into solid xenon in the range of 1.6 GPa$\leqslant p\leqslant$5.3 GPa.

Above 5.3 GPa at least two phases must be present, since the intensity ratio of ν_{Xe^*} and ν_{S1} changes when the laser is focused at a different spot in the sample space. No discontinuity of ν_{Xe^*} has been found at 5.3 GPa; therefore, this peak still corresponds to N_2 in solid Xe. As a consequence, the mole fraction of N_2 in S_1 is larger than 0.075. The frequency ν_{S1} is considerably lower than the Raman frequencies ν_{β^*} and ν_F. Therefore, it is concluded that S_1 is different from these two phases. A stoichiometric compound is proposed for S_1 for the following reasons. Taking into account the intensity of the Raman peaks and the position of the other phase lines as proposed in Fig. 11, the mole fraction of xenon in this phase is probably between 0.4 and 0.7. The only candidate structures for a disordered solid of the pure components are the ε phase of nitrogen (in pure nitrogen above 23 GPa) and the high-pressure intermediate close-packed phase in xenon (above 14 GPa at room temperature).[26] We have shown already that less than 7.5% nitrogen dissolves into fcc xenon; thus, it is unlikely that in the closely related close-packed structure the solubility will be much higher. The ε phase of N_2 is also not a good candidate for the following reasons. First, argon, which has nearly the same size as nitrogen, hardly dissolves into ε-N_2. Second, the transition line of the ε^* phase must shift from 23 to 5.3 GPa. Third, the frequency of ε^* must shift 4.6 cm^{-1}, while the frequency of δ^* is hardly shifted. Fourth, the Raman spectrum of ε-N_2 has two peaks, while only one peak is observed for S_1.

Ne-N_2

The first conclusion is that the solubility of nitrogen in solid neon is very low, if there is any solubility at all, as shown before. Then, since the spectrum of β^* is only shifted by 0.2 cm^{-1} compared to that of pure β-N_2, it is proposed that the β^* phase is a disordered solid of neon dissolved into β-N_2. The β^*-δ^* transition is shifted by 1.4 GPa to higher pressures for $x=0.90$, and therefore neon dissolves into this phase. Since the β^* phase coexists with a fluid phase for $x=0.90$, it is concluded that less than 10% neon dissolves into the β^* phase.

When the pressure is increased, the amount of fluid decreases and, on the neon-rich side of the phase diagram, the concentration of the fluid phase shifts to higher nitrogen contents and vice versa as shown in Fig. 12. For $x=0.052$ and $x=0.90$, this should result in a rapid increase of the FWHM as a function of pressure above the solid-fluid transition point, since the FWHM of the homogeneous fluid phase with $x=0.35$ is much higher than that with $x=0.052$ and $x=0.90$. This is indeed observed (Fig. 6). Moreover, the slope of ν_F versus the pressure should decrease for $x=0.052$ and $x=0.35$, and increase for $x=0.9$. This is observed as well (Fig. 5).

For the mixture with $x=0.052$, the mode ν_F disappears at the same pressure at which the modes of S_2 appear. Thus the mole fraction of S_2 is greater than 0.052. The mixture with $x=0.35$ shows both the Raman modes of S_2 and δ^*, while for $x=0.052$ the modes of δ^* have not been measured. This proves that the mole fraction of S_2 is between 0.052 and 0.35. Because the frequencies of S_2 deviate from the Raman

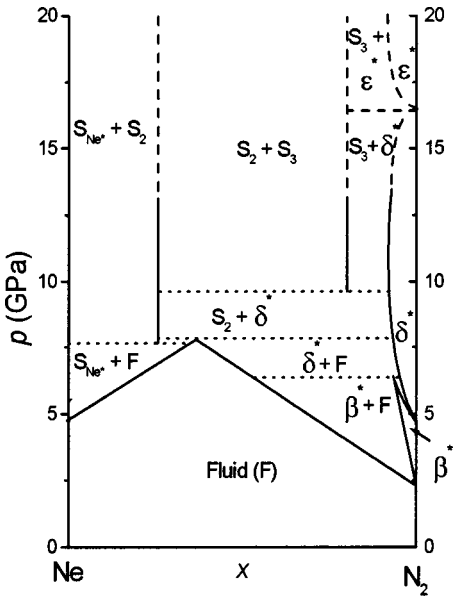

FIG. 12. Suggested p-x phase diagram for Ne-N_2 at 296 K.

modes of pure nitrogen and because the amount of neon that dissolves into the ε and δ phases is less than 10% as will be explained below, S_2 must be a new solid phase. The peak positions and the integrated intensity ratio of $\nu_{S2,a}$ and $\nu_{S2,b}$ have the same value for the two mixtures mentioned above: thus, it is proposed that S_2 is a van der Waals compound.

The fact that the modes of δ^* have the same frequency as pure δ-N_2 (Fig. 5) strongly suggests that the structure of δ^* is very similar to δ-N_2. However, the decrease of the intensity ratio of $\nu_{1\delta*}$ and $\nu_{2\delta*}$ from 0.33 for pure N_2 to 0.24 ± 0.03 for the mixtures suggests that the neon atoms dissolve into δ-N_2 and that they are mainly positioned at the a sites. Considering the intensity ratio, the neon mole fraction of δ^* must be 0.05 or higher. Since also for $x=0.90$ the Raman frequencies of δ^* and S_2 have been measured simultaneously in the scan of ν versus T, it is concluded that there is a coexistence region of δ^* and S_2 and that, therefore, the nitrogen mole fraction of δ^* is more than 0.90 in this region.

Because the intensity of the modes of δ^* changes with respect to that of S_3 when the laser is focused at a different spot in the sample space, it is concluded that δ^* and S_3 are two different solid phases. Since the spectrum of S_3 is different from that of the various solid phases of pure N_2, it can be either a van der Waals compound or a disordered solid of neon dissolved into N_2. As shown below, it cannot be a disordered solution of neon in ε-N_2. Although another disordered solid cannot be excluded, the van der Waals compound seems the most likely candidate because of the following arguments. The spectrum of S_3 is very similar to that of the van der Waals compound $He(N_2)_{11}$ as measured by Olijnyk and Jephcoat[16] and Scheerboom.[17] Analogous to the spectrum of the compound $He(N_2)_{11}$, the spectrum of S_3 shows three modes up to 15 GPa, $\nu_{S3,a}$ with about the same frequency as ν_1 of ε-N_2, $\nu_{S3,b}$ with a frequency slightly higher than ν_2 of ε-N_2, and $\nu_{S3,c}$ with a frequency slightly lower than ν_2 as shown in Fig. 5. In addition, also similar to the spectra of the compound $He(N_2)_{11}$, the intensity ratio of $\nu_{S3,a}$ and $\nu_{S3,b}$ is reduced compared to that of ν_1 and ν_2 of pure ε-N_2, and the mode $\nu_{S3,b}$ shows an asymmetry on the high-frequency side (marked by arrows in Fig. 8). There are no candidate structures for a disordered solid in neon, while in nitrogen there are only indications for a new phase η above 20 GPa at high pressure,[27] but this could not be confirmed in x-ray studies.[28] Most probably, η is only a small modification of the ε phase.

For $x=0.35$, a coexistence region of S_2 and S_3 has been found. Since the mole fraction of S_2 is less than 0.35, the mole fraction of S_3 must be more than 0.35. For $x=0.90$ no coexistence region of S_3 with S_2 has been observed, indicating that the mole fraction of S_3 is less than 0.9. For $x=0.9$, a coexistence region is proposed of S_3 with ε^* and δ^*, respectively. In the scan with $x=0.9$ of ν versus the temperature, up to 196 K the mode $\nu_{1\varepsilon*}$ has been found indeed, with the same frequency as ν_1 of pure ε-N_2. The Raman mode ν_2 of ε-N_2 has the same frequency as $\nu_{S3,b}$ within experimental accuracy, which explains why this mode could not be detected. Since the two modes $\nu_{S3,b}$ and $\nu_{2\varepsilon*}$ cannot be distinguished, the intensity ratio between $\nu_{1\varepsilon*}$ and $\nu_{2\varepsilon*}$ cannot be determined, and therefore it is impossible to draw conclusions on the solubility of Ne in ε-N_2. At 212 K the mode $\nu_{1\varepsilon*}$, observed at 196 K and lower temperatures, is no longer observed in the temperature scan for $x=0.9$. Therefore, it is proposed that for these temperatures S_3 coexists with δ^*. In pure N_2, the ε-δ transition occurs at 208 K at this particular pressure, and thus, within experimental accuracy, the ε^*-δ^* transition is not shifted for the mixture. Because S_3 has been found in coexistence with ε^* as well as with δ^*, it cannot be a disordered solid of neon dissolved in the ε or δ phase of nitrogen. Since the frequencies $\nu_{S3,a}$ and $\nu_{S3,b}$ are the same as ν_1 and ν_2 of δ-N_2, respectively, it is impossible to distinguish between these four peaks. The intensity ratio of $\nu_{S3,a}$ and $\nu_{S3,b}$ and that of $\nu_{S3,c}$ and $\nu_{S3,b}$ changes when the laser is focused at a different spot in the sample space, and in addition the ratio is higher than for $x=0.35$. These observations are in agreement with a δ^*-S_3 coexistence region, since the intensity ratio for δ^* is higher than that of S_3. This also explains the behavior of the spectra as a function of pressure for $x=0.90$ at and above 11.0 GPa at room temperature. Depending on the position of the laser spot, in the sample space we have found the modes of S_3, the modes of δ^*, or both.

DISCUSSION AND CONCLUSIONS

The high-pressure phase diagrams of Xe-N_2 and Ne-N_2 show a rich variety of solid phases. The present measurements show that the ratio of the diameters of the molecules, α, is only a very rough indication of the phase behavior of binary molecular systems. There is no solubility of the large nitrogen molecules in solid neon ($\alpha=0.74$), in agreement with theoretical predictions on hard-sphere systems. On the other hand, the small neon molecules do dissolve into the β^* and δ^* phases of N_2, even though the diameter ratio α is much smaller than 0.85. This results in a considerable deviation of the Hume-Rothery rule. The system Xe-N_2 shows indeed mutual solubility, as expected on the basis of the diameter ratio ($\alpha=0.89$), but in contrast to the computer simulations on hard-sphere systems, there is a larger solubility of the larger xenon molecules in nitrogen than vice versa. Therefore, the van der Waals interaction, the anisotropy, ori-

entational degrees of freedom, and the Coulomb forces probably play an important role in the mutual solubility in molecular solids at high pressure.

As discussed before, the Ne and Xe atoms dissolve substitutionally into δ-N_2. Analogous to the system Ar-N_2,[18,19] the Ne and Xe atoms have a preference for the *a* sites. The intensity of the ν_1 vibron is more reduced in the system Ne-N_2 than in the system Xe-N_2, although the maximum solubility is in the order of 10% for Ne-N_2 and more than 16% for Xe-N_2. Thus the Ne atoms have a stronger preference for the *a* sites than the Xe atoms.

In this work it was found that for Ne-N_2 the δ^*-β^* transition is shifted to higher pressures, just like Ar-N_2, while for Xe-N_2 the δ^*-β^* transition is shifted to slightly lower pressures. For the system Ne-N_2 the ε-δ transition is not shifted, in contrast to He-N_2 and Ar-N_2 where it is shifted to lower and higher pressures, respectively.

In Xe-N_2 one van der Waals compound S_1 has been found, while in Ne-N_2 ($\alpha=0.74$) at least two compounds exist: S_2 and S_3. The spectrum of S_2 consists of two distinct peaks, suggesting that the N_2 molecules are positioned on at least two distinct sites. The spectrum of S_3 is very similar to that of $He(N_2)_{11}$. Analogous to the interpretation of Olijnyk and Jephcoat[16] for $He(N_2)_{11}$, a close relation is proposed between the structure of S_3 and ε-N_2 and the Ne atoms may substitute or displace the N_2 molecules on the *a* sites.

Previously, the following compounds have been found in molecular systems: $A_{11}B$ (N_2-He,[15] $\alpha=0.62$), A_2B (CH_4-H_2,[9] $\alpha=0.72$), AB [CH_4-H_2 (Ref. 9)] AB_2 [Ne-He,[29] $\alpha=0.83$; Ar-H_2,[30] $\alpha=0.80$; CH_4-H_2 (Ref. 9)] and AB_4 [CH_4-H_2 (Ref. 9)], with *B* the smaller molecule. In computer simulations and analytical theories on hard-sphere systems, only AB, AB_2, and AB_{13} were found to be stable for $0.2 \leqslant \alpha \leqslant 0.42$, $0.42 \leqslant \alpha \leqslant 0.59$, and $0.54 \leqslant \alpha \leqslant 0.61$, respectively. AB_{13} has not been found in molecular systems, and although AB_2 and AB have been detected, the structure which has been determined experimentally for all compounds is different from the stable structure for hard-sphere systems. Because of the large discrepancy between hard-sphere and molecular systems, it is concluded that compound formation in molecular systems is not only determined by hard-sphere packing considerations. Just as in the case of disordered solids, the van der Waals interaction, the anisotropy, orientational degrees of freedom, and the Coulomb forces probably play an important role in the compound formation at high pressure.

Free energy calculations[29,31,32] with realistic potentials in the local harmonic approximation show that the compound $Ne(He)_2$ with the Laves structure is stable. Contrary to the hard-sphere systems, in the free energy calculations, the energy is the driving force for the compound formation.[32] Therefore, it can be concluded that good potentials are needed to understand the formation of van der Waals compounds.

The mole fraction of S_1 in the system Xe-N_2 is most probably $0.4 \leqslant x \leqslant 0.7$. Therefore, the most plausible structures for S_1 in Xe-N_2, are $(N_2)Xe$ with $x=0.5$ and $(N_2)_2Xe$, with $x=0.67$. The mole fraction of S_2 in the system Ne-N_2 is $0.052 \leqslant x \leqslant 0.35$. Therefore, we suggest that S_2 has the structure $N_2(Ne)_2$ with $x=0.33$, $N_2(Ne)_4$ with $x=0.2$, or $N_2(Ne)_{13}$ with $x=0.07$. The mole fraction of S_3 is probably $0.6 \leqslant x \leqslant 0.9$, and the similarity of the spectrum with that of $He(N_2)_{11}$ suggests that the number of N_2 molecules in the unit cell is large compared to the number of Ne atoms. The real structures can only be obtained with x-ray diffraction.

The frequency shift as a function of concentration can be explained for both systems by the following arguments. In the fluid phase the frequency increases at increasing Ne and decreasing Xe concentrations, respectively, due to the change in dispersive contribution.[33] In the solid phase, in addition to the dispersive contribution, the structure influences the shift. In contrast to the fluid phase, in the δ^* phase neither for Xe-N_2 nor for Ne-N_2 has a shift been detected for the frequency with respect to pure δ-N_2, while the solubility of Xe in this phase is larger than 16 mol %. This may partly be explained by the peculiar structure of δ-N_2. The Xe and Ne atoms have a preference for the *a* sites. Since the first neighbors of molecules on both the *a* sites and *c* sites are *c* sites, the nearest neighbors of N_2 molecules in the mixed solids are N_2 molecules. Preliminary simulations[34] show that in this case the dispersive contribution is not very sensitive to the composition. The ε phase is obtained from the δ phase by a small distortion. Therefore, the same arguments might explain why the frequency of S_3 in Ne-N_2 is only slightly shifted as compared to that in pure ε-N_2. In Xe-N_2, the mode ν_{Xe^*}, with a mole fraction lower than 0.075, has a much lower frequency than that in pure N_2. The decrease in the frequency is so large that it cannot be attributed only to a change in the dispersive contribution. In Ref. 35 it is shown that because Xe crystallizes on a larger grid than N_2, the axial force exerted on the N_2 molecules in solid Xe is lower than that in pure N_2, resulting in an additional decrease in the frequency.

*Electronic address: ekooi@wins.uva.nl
†Electronic address: schouten@wins.uva.nl

[1] W. Hume-Rothery, G. W. Mabbott, and K. M. Channel-Evans, Philos. Trans. R. Soc. London, Ser. A **233**, 1 (1934).
[2] W. G. T. Kranendonk and D. Frenkel, J. Phys.: Condens. Matter **1**, 7735 (1989); Mol. Phys. **72**, 679 (1991); D. Kofke, Mol. Simul. **7**, 285 (1991).
[3] F. Lutsko and B. Baus, Phys. Rev. Lett. **64**, 761 (1990); J. L. Barrat, M. Baus, and J. P. Hansen, J. Phys. C **20**, 1413 (1987); X. C. Zeng and D. W. Oxtoby, J. Chem. Phys. **93**, 4357 (1990); A. R. Denton and N. W. Ashcroft, Phys. Rev. A **42**, 7312 (1990).
[4] X. Cottin and P. A. Monson, J. Chem. Phys. **99**, 8914 (1993).
[5] M. D. Eldridge, P. A. Madden, and D. Frenkel, Nature (London) **365**, 35 (1993); Mol. Phys. **79**, 105 (1993); **80**, 987 (1993).
[6] M. J. Murray and J. V. Sanders, Philos. Mag. A **42**, 721 (1980).
[7] H. Xu and M. Baus, J. Phys.: Condens. Matter **4**, L663 (1992).
[8] X. Cottin and P. A. Monson, J. Chem. Phys. **102**, 3354 (1995).
[9] M. S. Somayazulu, L. W. Finger, R. J. Hemley, and H. K. Mao, Science **271**, 1400 (1996).
[10] J. A. Schouten and M. E. Kooi, in *High Pressure Molecular Science, NATO Advanced Study Institute, Series B: Physics*, edited by R. Winter and J. Jonas (Kluwer Academic, Dordrecht, 1999), pp. 187–204.

[11] Y. A. Freiman and M. A. Strzhemechny, in *Physics of Cryocrystals*, edited by V. G. Manzheli and Y. A. Freiman (AIP, Woodbury, NY, 1997), pp. 286–364.
[12] M. I. M. Scheerboom and J. A. Schouten, Phys. Rev. Lett. **71**, 2252 (1993); M. Hanfland, M. Lorenzen, C. Wassilew-Reul, and F. Zontone, Rev. High Pressure Sci. Technol. **7**, 787 (1998); A. Mulder, J. P. J. Michels, and J. A. Schouten, Phys. Rev. B **57**, 7571 (1998).
[13] W. L. Vos and J. A. Schouten, Phys. Rev. Lett. **64**, 898 (1990).
[14] M. I. M. Scheerboom and J. A. Schouten, J. Phys.: Condens. Matter **3**, 8305 (1991).
[15] W. L. Vos, L. W. Finger, R. J. Hemley, J. Z. Hu, H. K. Mao, and J. A. Schouten, Nature (London) **358**, 46 (1992).
[16] H. Olijnyk and A. P. Jephcoat, J. Phys.: Condens. Matter **9**, 11219 (1997).
[17] M. I. M. Scheerboom, Ph.D. thesis, University of Amsterdam, 1996.
[18] T. Westerhoff and R. Fiele, Phys. Rev. B **54**, 913 (1996).
[19] M. E. Kooi and J. A. Schouten, Phys. Rev. B **57**, 10 407 (1998).
[20] E. P. van Klaveren, J. P. J. Michels, and J. A. Schouten, J. Low Temp. Phys. **111**, 413 (1998).
[21] H. K. Mao, J. Xu, and P. M. Bell, J. Geophys. Res. **91**, 4673 (1986).
[22] W. L. Vos and J. A. Schouten, J. Appl. Phys. **69**, 6744 (1991).
[23] J. P. J. Michels, M. E. Kooi, and J. A. Schouten, J. Chem. Phys. **108**, 2695 (1998).
[24] W. L. Vos and J. A. Schouten, J. Chem. Phys. **91**, 6302 (1989).
[25] P. H. Lahr and W. G. Eversole, J. Chem. Eng. Data **7**, 42 (1962).
[26] A. P. Jephcoat, H.-k. Mao, L. W. Finger, D. E. Cox, R. J. Hemley, and C.-s. Zha, Phys. Rev. Lett. **59**, 2670 (1987).
[27] R. Reichline, D. Schiferl, S. Martin, C. Vanderborgh, and R. L. Mills, Phys. Rev. Lett. **55**, 1464 (1985).
[28] H. Olijnyk, J. Chem. Phys. **93**, 8968 (1990).
[29] P. Loubeyre, M. Jean-Louis, R. LeToullec, and L. Charon-Gérard, Phys. Rev. Lett. **70**, 178 (1993).
[30] P. Loubeyre, R. LeToullec, and J.-P. Pinceaux, Phys. Rev. Lett. **72**, 1360 (1994).
[31] J.-L. Barrat and W. L. Vos, J. Chem. Phys. **97**, 5707 (1992).
[32] W. L. Vos and J. A. Schouten, Fiz. Nizk. Temp. **19**, 481 (1993) [Low Temp. Phys. **19**, 338 (1993)].
[33] M. I. M. Scheerboom, J. P. J. Michels, and J. A. Schouten, J. Chem. Phys. **104**, 9388 (1996).
[34] J. P. J. Michels (private communication).
[35] M. E. Kooi, J. P. J. Michels, and J. A. Schouten, J. Chem. Phys. **110**, 3023 (1999).
[36] M. I. M. Scheerboom and J. A. Schouten, J. Chem. Phys. **105**, 2553 (1996).
[37] W. L. Vos and J. A. Schouten, J. Chem. Phys. **94**, 3835 (1991).